Model-independent constraints on leptoquarks from rare μ and τ lepton processes

Emidio Gabrielli*
Departamento de Física Teórica, C-XI, Instituto de Física Teórica, C-XVI, Universidad Autónoma, E-28049 Madrid, Spain
(Received 10 December 1999; published 1 August 2000)

We perform a model-independent analysis so as to constrain the leptoquark (LQ) models from negative searches for $\mu\to e\gamma$, $\mu\to 3e$ decays (and analogous processes in the τ sector), and coherent μ-e conversion in nuclei. We considerably improve some constraints obtained by analyses known in the literature, analyses which we show have by far underestimated the LQ contributions to the $\mu\to 3e$. In particular we find that the coherent μ-e conversion in nuclei mediated by the photon-conversion mechanism and the $\mu\to 3e$ decay are golden plates where the flavor-changing leptoquark couplings, involving the second and third quark generations, can be strongly constrained. This is due to the fact that these processes get the enhancements by large $\log(m_q^2/m_{\rm LQ}^2)$ terms which are induced by the so-called ''photon-penguin'' diagrams. These enhancements, which produce a mild Glashow-Iliopoulos-Maiani (GIM) suppression in the amplitudes, have not been taken into account in the previous analyses. We show that the $\mu\to e\gamma$ decay can set weaker constraints on the LQ models and this is because its amplitude is strongly GIM suppressed by the terms of order $O(m_q^2/m_{\rm LQ}^2)$. We also present the results for the corresponding constraints in the τ sector. Finally, the prospects of the future muon experiments for the improvement of the present bounds are analyzed and discussed.

PACS number(s): 12.60.−i, 13.35.Bv, 13.35.Dx

I. INTRODUCTION

The leptoquark (LQ) color triplet bosons, predicted by grand unified theories [1], superstring inspired E_6 [2,3], compositeness [4], and technicolor models [5], have been the subject of numerous phenomenological investigations. The main direct experimental searches for LQs investigate their production in the s channel [2,6]; these searches are carried out at the $e-p$ collider HERA at DESY [6,7]. On the other hand, the indirect searches of LQs consist mainly of analyzing the anomalous effects induced by the LQ interactions in deep inelastic scattering as well as in low energy processes [8–10].

Recently there has been a renewed interest in the subject [11] due to the high Q^2 anomalous events observed in the H1 [12] and ZEUS [13] experiments at HERA, although subsequent analyses of new data have shown a less significant discrepancy with the standard model (SM) predictions [14].

In the literature [1–4], predictions are given for the existence of two types of LQs: the scalar and vectorial ones. In the present article we perform a model-independent study of the LQs, and, in particular, we restrict ourselves to the most general renormalizable interactions, which conserve the baryon (B) and lepton (L) number, and which are compatible with the SM symmetries [6]. Therefore, in the case of vectorial LQs, we consider only the gauge-vectorial ones. From a theoretical point of view there is no reason to believe that the quark-lepton couplings, mediated by LQ interactions, are simultaneously diagonalizable with the quark and lepton mass matrices. As a consequence, both scalar and vectorial LQs can generate, when integrated out, effective flavor-changing (FC) interactions between quarks and leptons of the form [8–10]

$$\frac{\lambda_{\rm LQ}^{ni}\lambda_{\rm LQ}^{\dagger jm}}{m_{\rm LQ}^2}(\overline{q^i}\gamma_\mu P^q q^j)(\overline{l^m}\gamma_\mu P^l l^n),$$

$$\text{and/or,}\quad \frac{\lambda_{\rm LQ}^{ni}\lambda_{\rm LQ}^{\dagger jm}}{m_{\rm LQ}^2}(\overline{q^i}P^q q^j)(\overline{l^m}P^l l^n), \tag{1}$$

where $m_{\rm LQ}$ indicates the LQ mass and the chiral projectors P^q and P^l of the quarks and lepton, respectively, can be left [$P_L=(1-\gamma_5)/2$] or right [$P_R=(1+\gamma_5)/2$]. Since these effective interactions can be generated even at tree-level, strong constraints on the LQ couplings $\lambda_{\rm LQ}^{ij}$ and masses can be set by the flavor changing neutral current (FCNC) processes. In particular, strong constraints on LQ models are obtained by means of the rare FC K, D, and B meson decays [9,10] as well as in the leptonic sector [10]. In this framework in Ref. [10] a model-independent analysis was performed to constrain the masses and couplings of the LQs (B and L conserving).

In the present article we carry out a detailed analysis of the LQ contributions to the μ and τ leptonic rare processes. Since we do not consider the CP violating processes where the imaginary parts of $\lambda_{\rm LQ}^{ij}$ couplings are better constrained, we assume, as in Ref. [10], that all the couplings $\lambda_{\rm LQ}^{ij}$ are real. In addition we require that all the couplings $\lambda_{\rm LQ}^{ij}$ should be unitary[1] in both vector and scalar LQ sectors. This last

[1]Note, however, that unitary LQ couplings can naturally appear in some ''minimal'' models where the LQ interactions are assumed to be universal (in flavor) in the basis of the quark and lepton SM gauge-eigenstates. This is, for example, the case of the gauge-vectorial LQs which appear in the gauge multiplet of the standard grand unified theories (GUTs) [1]. Then, after rotating the quark and lepton fields into the corresponding mass-eigenstates, unitary flavor-changing LQ couplings should appear in the interactions in Eq. (2) being proportional to the products of the (unitary) diagonalization matrices of the quark and lepton mass matrices.

*Electronic address: emidio.gabrielli@cern.ch, emidio.gabrielli@uam.es

assumption will give us conservative limits. Indeed the unitarity of the LQ couplings makes active a Glashow-Iliopoulos-Maiani-(GIM)–type mechanism in some FCNC processes, such as, for example, $\mu\to e\gamma$, $\tau\to e\gamma$ decay, K-$\bar{K}$, or B-$\bar{B}$ mixing, which naturally suppresses the potentially large LQ contributions. We recall that the limits obtained in Ref. [10] (from $\mu\to e\gamma$ or $\tau\to e\gamma$) in the scalar sector are less conservative than ours since the authors of Ref. [10] assumed unitary couplings only in the gauge-vectorial sector.

Within the class of interesting processes, used to constrain the LQ models in the leptonic sector, a special role is played by the rare FC violating decays $\mu\to e\gamma$ and $\mu^-\to e^-e^-e^+$ ($\mu\to 3e$) [10] and analogous processes in the τ sector, and the coherent $\mu-e$ conversion in nuclei [17–22] (in the following for the $\mu-e$ conversion we always mean the coherent process). The last of these processes is used to set the strongest constraints on the combination $\lambda_{\rm LQ}^{21}\lambda_{\rm LQ}^{11}/m_{\rm LQ}^2$ for both the vectorial and scalar LQs which involve the first generation of quarks, since, in this case, the effective Hamiltonian is induced at tree-level. On the contrary the $\mu\to e\gamma$ and $\mu\to 3e$ decays, which are induced at one-loop, allow us to constrain the complementary combinations on couplings and masses involving the second and third generation of quarks, namely $\lambda_{\rm LQ}^{2i}\lambda_{\rm LQ}^{1i}/m_{\rm LQ}^2$ or $\sqrt{\lambda_{\rm LQ}^{2i}\lambda_{\rm LQ}^{1i}}/m_{\rm LQ}^2$, where $i=2,3$. In this respect the authors of Ref. [10] found that the radiative muon decay $\mu\to e\gamma$ is better than the $\mu\to 3e$ process in setting stronger bounds on these combinations of couplings.

One of the aims of this paper is to show that the conclusions of Ref. [10] do not hold when the unitarity of the LQ couplings is required in both scalar and vectorial LQ sectors and the dominant diagrams (not included in Ref. [10]) are taken into account in the $\mu\to 3e$ decay. At the one-loop level the LQs give contributions to the $\mu\to e\gamma$ decay by means of the so-called magnetic-penguin diagrams shown in Fig. 1(d) and 1(e)]. In Ref. [10] it is found that the $\mu\to e\gamma$ amplitude, mediated by scalar LQs (which couple to the external leptons with the same chirality), is enhanced with respect to the one corresponding to the gauge-vectorial LQs, since these last ones are strongly GIM suppressed by terms of order $m_q^2/m_{\rm LQ}^2$ (where m_q is the typical quark mass running in the loop). As a consequence they show that the scalar LQ couplings and masses are more strongly constrained than the corresponding vectorial ones. In the present work we prove that, when the unitarity for the LQ couplings is extended to the scalar sector, the scalar LQ contribution to the $\mu\to e\gamma$ decay's amplitude is significantly suppressed by the GIM mechanism so that it turns out to be of the same order of the gauge-vectorial one. This in particular implies that the constraints on scalar LQ couplings, which we find coming from the $\mu\to e\gamma$ decay, are weaker than the corresponding ones given in Ref. [10] and are roughly of the same order of the gauge-vectorial ones.

In addition we find that in Ref. [10] the main contribution of diagrams to the $\mu\to 3e$ decay has been underestimated. The main purpose of this paper, however, is to show that the $\mu\to 3e$ process is more powerful than the $\mu\to e\gamma$ one in setting strong bounds on mass and couplings of scalar and gauge-vectorial LQs. (We will see that similar considerations hold for the analogous decays in the τ sector.) This result can be simply understood as follows. The main contribution of diagrams to the $\mu\to 3e$ decay derives from the so-called photon-penguins [see Figs. 1(a) and 1(b)] which were not taken into account in Ref. [10]. In the large LQ mass ($m_{\rm LQ}$) limit (with respect to the quark mass m_q) the photon-penguins, since they are proportional to $\log(m_q/m_{\rm LQ})$, are only ''mildly'' GIM suppressed (instead of being ''strongly'' GIM suppressed as the box and Z-penguin diagrams are). This means that to have an extra electromagnetic coupling α in the $\mu\to 3e$ rate (with respect to the $\mu\to e\gamma$ one) is a more convenient price to pay than the price of the $O(m_q^4/m_{\rm LQ}^4)$ suppression in the $\mu\to e\gamma$ rate in setting stronger bounds. These log enhancements in $\mu\to 3e$ were known in the literature [15] for certain models (and more recently analyzed in the context of effective theories [16]); however, they were not applied in this context. In fact the authors of Ref. [10], in order to simplify the analysis, only consider the contribution of the box diagrams to the $\mu\to 3e$ decay [which are of the order $O(\lambda_{\rm LQ}^4 m_q^2/m_{\rm LQ}^4)$] and this resulted in underestimating the branching ratio.

The photon-penguin diagrams also give a relevant contribution to the μ-e conversion in nuclei [17–22] via the photon-conversion mechanism. The log enhancement of these diagrams will enable us to show that the μ-e conversion in nuclei is another golden-plate process which sets strong bounds for LQ couplings involving the second and third quark generations. These bounds could turn out to be more competitive than the corresponding ones obtained from the $\mu\to 3e$ process. However, we stress that the bounds from the μ-e conversion suffer the problem of being model-dependent due to the nonperturbative calculations of the nuclear form factors, while the bounds coming from the $\mu\to 3e$ decay are not.

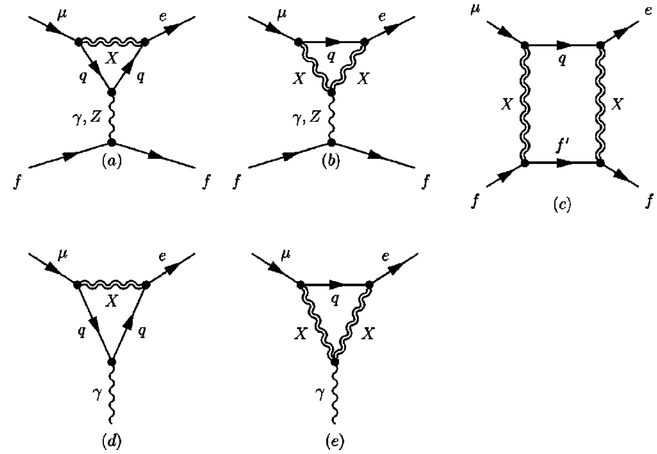

FIG. 1. The photon (γ)- and Z-penguin (a), (b) and the box (c) diagrams for the $\mu\to e f\bar{f}$ process, and the magnetic-penguin (d), (e) diagrams for the $\mu\to e\gamma$ process, in the LQ model, where f, q, and X indicate a general external fermion, quarks and LQs, respectively. In addition to (a), (b) there are also the diagrams with the self-energy insertions (not included in this figure), where the γ or Z is attached on the external e and μ, which contribute to the $\mu\to e f\bar{f}$ amplitude.

The interesting aspects of the photon-penguin diagrams, which give universal contributions to the $\mu\to 3e$ and μ-e conversion processes, is that these log enhancements appear in both the scalar and vectorial LQ exchanges which have the same chirality couplings with the external leptons. We shall see that this property enables us to set strong bounds in both the scalar and vectorial LQ sectors.

The same considerations regarding the log enhancements hold for the $\tau\to 3e$, $\tau\to 3\mu$, $\tau\to e\mu^+\mu^-$, and $\tau\to\mu e^+e^-$ processes. However, due to weaker experimental upper limits on the branching ratios, the constraints on the LQ couplings and masses, which come from these rare processes, are not as strong as they are in the μ sector.

The paper is organized as follows. In Sec. II we present the analytical results for the LQ contributions (in the large LQ mass limit) to the branching ratios of $\mu\to e\gamma$, and in Sec. III we give the corresponding results for $\mu\to 3e$ decay and $\mu-e$ conversion. In Sec. IV we present the numerical results for bounds on the combination of LQ couplings and masses constrained by the experimental upper limits on $\mu\to e\gamma$, $\mu\to 3e$ decay (and analogous processes in the τ sector), and the $\mu-e$ conversion. Finally, the last section is devoted to our conclusions.

II. $\mu\to e\gamma$ DECAY

In the present section we give the main results for the relevant LQ contributions to the total branching ratio of $\mu\to e\gamma$. We begin our analysis by fixing the conventions for the most general renormalizable Lagrangian for scalar and gauge-vectorial LQ interactions (from now on, if not strictly necessary, we will omit the suffix gauge in the vectorial LQ). This Lagrangian, which is B and L conserving and invariant under the $SU(3)_c\otimes SU(2)_L\otimes U(1)$ symmetry group of the SM, was first proposed in Ref. [6]. Its expression, in the notation of Ref. [10], is given by

$$\begin{aligned}\mathcal{L}_S=&\{(\lambda_{LS_0}\overline{q_L^c}\imath\tau_2 l_L+\lambda_{RS_0}\overline{u_R^c}e_R)S_0^\dagger+(\lambda_{R\tilde{S}_0}\overline{d_R^c}e_R)\tilde{S}_0^\dagger\\&+(\lambda_{LS_{1/2}}\overline{u_R}l_L+\lambda_{RS_{1/2}}\overline{q_L}\imath\tau_2 e_R)S_{1/2}^\dagger+(\lambda_{L\tilde{S}_{1/2}}\overline{d_R}l_L)\tilde{S}_{1/2}^\dagger\\&+(\lambda_{LS_1}\overline{q_L^c}\imath\tau_2\tau^i l_L)S_1^i\}+\text{H.c.},\\\mathcal{L}_V=&\{(\lambda_{LV_0}\overline{q_L}\gamma_\mu l_L+\lambda_{RV_0}\overline{d_R}\gamma_\mu e_R)V_0^{\dagger\mu}+(\lambda_{R\tilde{V}_0}\overline{u_R}\gamma_\mu e_R)\tilde{V}_0^{\mu\dagger}\\&+(\lambda_{LV_{1/2}}\overline{d_R^c}\gamma_\mu l_L+\lambda_{RV_{1/2}}\overline{q_L^c}\gamma_\mu e_R)V_{1/2}^{\mu\dagger}\\&+(\lambda_{L\tilde{V}_{1/2}}\overline{u_R^c}\gamma_\mu l_L)\tilde{V}_{1/2}^{\mu\dagger}+(\lambda_{LV_1}\overline{q_L}\gamma_\mu\tau^i l_L)V_1^{\mu i\dagger}\}+\text{H.c.},\end{aligned}\tag{2}$$

where $\mathcal{L}_S$ and $\mathcal{L}_V$ contain the interactions with the scalar (S_0, $\tilde{S}_0$, $S_{1/2}$, $\tilde{S}_{1/2}$ S_1^i) and vectorial (V_0^μ, $\tilde{V}_0^\mu$, $V_{1/2}^\mu$, $\tilde{V}_{1/2}^\mu$, $V_1^{i\mu}$) LQs fields, respectively. The subscript (0,1/2,1) in each scalar and vectorial LQ indicates the *singlet*, *doublet*, and *triplet* $SU(2)_L$ representation, respectively, whereas the τ^is are the Pauli matrices. The quark fields $q^c_{L,R}$ are the corresponding conjugate of the $q_{L,R}$ fields, respectively, where $q^c_{L,R}\equiv(P_{L,R}q)^c$. Note that the generation (flavor) and color indices in the fields appearing in Eq. (2) are omitted. As we pointed out in the Introduction, we assume that all the scalar and vectorial LQ couplings λ_{LQ} are unitary (in the flavor space) in the basis of the quark and lepton mass eigenstates, and that the LQs do not carry flavor indices. Moreover, since we do not consider the CP violating processes in our analysis, we assume that all the couplings are real.

The relevant (gauge-invariant) effective Hamiltonian for the $\mu\to e\gamma$ decay is given by

$$H=\frac{4G_F}{\sqrt{2}}(Q_{LR}C_{LR}+Q_{RL}C_{RL}),\tag{3}$$

where $Q_{LR}=\overline{e}_L\sigma_{\mu\nu}\mu_R F^{\mu\nu}$ and $Q_{RL}=\overline{e}_R\sigma_{\mu\nu}\mu_L F^{\mu\nu}$ are the magnetic-dipole operators, $F^{\mu\nu}$ is the electromagnetic field strength, and C_{LR}, C_{RL} are the corresponding Wilson coefficients.

The Wilson coefficients C_{LR}, C_{RL} receive their main contributions, at the electroweak scale, through one-loop magnetic penguin diagrams shown in Figs. 1(d) and 1(e). Since these diagrams are proportional to the $\sigma_{\mu\nu}$ form factor, one needs a chirality flip. In the SM, as the charged currents are only of the V-A type, one can get this chirality flip by means of an external mass insertion.[2] This imply that the C_{LR} and C_{RL} are proportional to the electron m_e and muon m_μ masses, respectively. However in the SM the Wilson coefficients C_{LR} and C_{RL} are strongly suppressed by the GIM mechanism which forces them to be proportional to m_ν^2/m_W^2 terms times the corresponding Cabibbo-Kobayashi-Maskawa (CKM) angles of the leptonic sector, with m_ν being the heaviest neutrino mass running in the loop.

We now consider the LQ contributions to the magnetic penguin diagrams [see Figs. 1(d), 1(e)]. These diagrams receive finite contributions from both the scalar and vectorial LQs interactions in Eq. (2). With respect to the SM diagrams, the W and neutrino internal lines are replaced by a LQ and quark, respectively, and an additional diagram (where the external photon is attached to the internal quark line) is included. The SM GIM suppression terms of order $O(m_\nu^2/m_W^2)$ are now replaced by $O(m_q^2/m_{\text{LQ}}^2)$, where m_{LQ} is a typical LQ mass running in the loop.

In order to find the constraints on the combination of LQ couplings and masses we impose, as in Ref. [10], that each individual LQ coupling contribution to the branching ratio does not exceed (in absolute value) the experimental upper limit on the branching ratio. Therefore, in order to simplify the analysis, we consider in the branching ratio only one single LQ coupling contribution each time; this is done by "switching off" all the other couplings. Moreover we as-

[2]In some extensions of the SM, such as the left-right-, the LQs-, and the supersymmetric-models (where the leptons or quarks can have both the left and right couplings to the new particles), this chirality flip can be realized by a heavy (internal) fermion mass insertion which turns out to give a strong chiral enhancement with respect to the SM amplitude.

sume that the LQ masses are larger than the quark ones (including the case of the top quark) so that we only take the leading contribution to the Wilson coefficients.

By means of the Lagrangian in Eq. (2), we give in the sequel the results for the total branching ratio $\mu\to e\gamma$, where only the contribution of a single LQ coupling is considered. By neglecting the terms of order $O(m_q^4/m_{\rm LQ}^4)$ in the Feynman diagrams we obtain the following.

Gauge-vectorial LQs:

$$
\begin{aligned}
B_R^{\lambda_{LV_0}} &= \frac{B_V}{m_{V_0}^8 G_F^2}\left(Q_D-\frac{Q_{V_0}}{2}\right)^2\left[\sum_{i=1}^{3}\lambda_{LV_0}^{2i}\lambda_{LV_0}^{1i}m_{D_i}^2\right]^2,\\
B_R^{\lambda_{RV_0}} &= B_R^{\lambda_{LV_0}}(\lambda_{LV_0}\to\lambda_{RV_0}),\\
B_R^{\lambda_{R\tilde V_0}} &= \frac{B_V}{m_{\tilde V_0^2}^8 G_F^2}\left(Q_U-\frac{Q_{\tilde V_0}}{2}\right)^2\left[\sum_{i=1}^{3}\lambda_{R\tilde V_0}^{2i}\lambda_{R\tilde V_0}^{1i}m_{U_i}^2\right]^2,\\
B_R^{\lambda_{LV_{1/2}}} &= \frac{B_V}{m_{V_{1/2}}^8 G_F^2}\left(Q_D+\frac{Q_{V_{1/2}^D}}{2}\right)^2\left[\sum_{i=1}^{3}\lambda_{LV_{1/2}}^{2i}\lambda_{LV_{1/2}}^{1i}m_{D_i}^2\right]^2,\\
B_R^{\lambda_{RV_{1/2}}} &= \frac{B_V}{m_{V_{1/2}}^8 G_F^2}\left[\sum_{q=U,D}\sum_{i=1}^{3}\lambda_{RV_{1/2}}^{2i}\lambda_{RV_{1/2}}^{1i}m_{q_i}^2\left(Q_q\right.\right.\\
&\quad\left.\left.+\frac{Q_{V_{1/2}^q}}{2}\right)\right]^2,\\
B_R^{\lambda_{L\tilde V_{1/2}}} &= \frac{B_V}{m_{\tilde V_{1/2}}^8 G_F^2}\left(Q_U+\frac{Q_{\tilde V_{1/2}^D}}{2}\right)^2\left[\sum_{i=1}^{3}\lambda_{L\tilde V_{1/2}}^{2i}\lambda_{L\tilde V_{1/2}}^{1i}m_{U_i}^2\right]^2,\\
B_R^{\lambda_{LV_1}} &= \frac{B_V}{m_{V_1}^8 G_F^2}\left[\sum_{i=1}^{3}\lambda_{LV_1}^{2i}\lambda_{LV_1}^{1i}\left(m_{D_i}^2\left(Q_D-\frac{Q_{V_1^3}}{2}\right)\right.\right.\\
&\quad\left.\left.+2m_{U_i}^2\left(Q_U-\frac{Q_{V_1^1}}{2}\right)\right)\right]^2.
\end{aligned}
\tag{4}
$$

Scalar LQs:

$$
\begin{aligned}
B_R^{\lambda_{LS_0}} &= \frac{B_S}{m_{S_0}^8 G_F^2}\left[\sum_{i=1}^{3}\lambda_{LS_0}^{2i}\lambda_{LS_0}^{1i}m_{U_i}^2\right.\\
&\quad\left.\times(Q_U\rho(x_{U_iS_0})-Q_{S_0})\right]^2,\\
B_R^{\lambda_{RS_0}} &= B_R^{\lambda_{LS_0}}(\lambda_{LS_0}\to\lambda_{RS_0}),\\
B_R^{\lambda_{R\tilde S_0}} &= \frac{B_S}{m_{\tilde S_0^2}^8 G_F^2}\left[\sum_{i=1}^{3}\lambda_{R\tilde S_0}^{2i}\lambda_{R\tilde S_0}^{1i}m_{D_i}^2\right.\\
&\quad\left.\times(Q_D\rho(x_{D_i\tilde S_0})-Q_{\tilde S_0})\right]^2,
\end{aligned}
$$

TABLE I. Electromagnetic charges of the scalar (S) and vectorial (V) LQs in unit of e.

LQ	$Q_{\rm LQ}$
S_0	$-1/3$
$\tilde S_0$	$-4/3$
$(S_{1/2}^U,\ S_{1/2}^D)$	$(-2/3,-5/3)$
$(\tilde S_{1/2}^U,\ \tilde S_{1/2}^D)$	$(1/3,-2/3)$
$(S_1^1,\ S_1^2,\ S_1^3)$	$(-4/3,2/3,-1/3)$
V_0	$-2/3$
$\tilde V_0$	$-5/3$
$(V_{1/2}^U,\ V_{1/2}^D)$	$(-1/3,-4/3)$
$(\tilde V_{1/2}^U,\ \tilde V_{1/2}^D)$	$(2/3,-1/3)$
$(V_1^1,\ V_1^2,\ V_1^3)$	$(1/3,-2/3,-5/3)$

$$
\begin{aligned}
B_R^{\lambda_{LS_{1/2}}} &= \frac{B_S}{m_{S_{1/2}}^8 G_F^2}\left[\sum_{i=1}^{3}\lambda_{LS_{1/2}}^{2i}\lambda_{LS_{1/2}}^{1i}m_{U_i}^2\right.\\
&\quad\left.\times(Q_U\rho(x_{U_iS_{1/2}})+Q_{S_{1/2}^D})\right]^2,\\
B_R^{\lambda_{RS_{1/2}}} &= \frac{B_S}{m_{S_{1/2}}^8 G_F^2}\left[\sum_{i=1}^{3}\lambda_{RS_{1/2}}^{2i}\lambda_{RS_{1/2}}^{1i}\right.\\
&\quad\times(m_{D_i}^2(Q_D\rho(x_{D_iS_{1/2}})+Q_{S_{1/2}^U})\\
&\quad\left.+m_{U_i}^2(Q_U\rho(x_{U_iS_{1/2}})+Q_{S_{1/2}^D}))\right]^2,\\
B_R^{\lambda_{L\tilde S_{1/2}}} &= \frac{B_S}{m_{\tilde S_{1/2}}^8 G_F^2}\left[\sum_{i=1}^{3}\lambda_{L\tilde S_{1/2}}^{2i}\lambda_{L\tilde S_{1/2}}^{1i}m_{D_i}^2(Q_D\rho(x_{D_i\tilde S_{1/2}})\right.\\
&\quad\left.+Q_{\tilde S_{1/2}^D})^2\right]^2,\\
B_R^{\lambda_{LS_1}} &= \frac{B_S}{m_{S_1}^8 G_F^2}\left[\sum_{i=1}^{3}\lambda_{LS_1}^{2i}\lambda_{LS_1}^{1i}\right.\\
&\quad\times(m_{U_i}^2(Q_U\rho(x_{U_iS_1})-Q_{S_1^3})\\
&\quad\left.+2m_{D_i}^2(Q_D\rho(x_{D_iS_1})-Q_{S_1^1}))\right]^2,
\end{aligned}
\tag{5}
$$

where $B_V=3\alpha N_c^2/(64\pi)$ and $B_S=\alpha N_c^2/(192\pi)$. $N_c=3$ is the number of colors and the function $\rho(x)=(11+6\log x)/2$, $x_{ab}=m_a^2/m_b^2$, $Q_U=2/3$, and $Q_D=-1/3$. For the values of the LQ charges $Q_{\rm LQ}$ the reader is referred to Table I. Note that the leading term in $m_q^2/m_{V_0}^2$ expansions in $B_R^{\lambda_{LV_0}}$, $B_R^{\lambda_{RV_0}}$ is zero due to the fact that $Q_D-Q_{V_0}/2=0$. Therefore the nonzero LQs contributions to these branching ratios is highly suppressed since they are of the order $O(m_q^8/G_F^2m_{V_0}^{12})$.

We stress that our findings for the analytical expressions in Eq. (5), due to different assumptions in the scalar LQ couplings sector, is somewhat different than the corresponding one in Ref. [10]. Indeed, in Ref. [10], only the terms at the zero order in the quark mass expansion give the leading scalar LQ contribution to $\mu\to e\gamma$. However, in our case, when the sum over the quark generations is performed, these terms vanish due to the unitarity of the $\lambda_{\rm LQ}$ matrices and survive only the next-to-leading ones which are suppressed by terms of order $O(m_q^2/m_{\rm LQ}^2)$. We check that our results are consistent with the analogous calculations obtained, for example, from the charged Higgs boson and supersymmetric contributions to the $b\to s\gamma$ amplitude [23].

Since the doublet LQs can have both couplings λ_L and λ_R (with left and right chiralities, respectively), one can get a chiral enhancement in the $\mu\to e\gamma$ amplitude by flipping the chirality with an internal (heavy) quark mass insertion in contrast with the external muon mass. In this case the resulting amplitude has to be proportional to $\lambda_L\lambda_R$. However, in the present paper we do not analyze the constraints on this combination of couplings. Indeed we follow the usual approach, (adopted also in Ref. [10]), in setting more conservative bounds and, more precisely, consider only the effects of the same kind of coupling constant per time while ''switching off'' all the others.

In the τ sector the corresponding analytical results for the $\tau\to e\gamma$ and $\tau\to\mu\gamma$ decays are simply obtained by making the following substitutions in the right-hand sides (r.h.s.) of the branching ratios $B_R^{\lambda_{\rm LQ}}(\mu\to e\gamma)$ in Eqs. (4), (5),

$$B_R^{\lambda_{\rm LQ}}(\tau\to e\gamma)=B_R^{\rm exp}(\tau^-\to\mu^-\overline{\nu}_\mu\nu_\tau)\times B_R^{\lambda_{\rm LQ}}(\mu\to e\gamma)\times\{\lambda_{\rm LQ}^{2i}\lambda_{\rm LQ}^{1i}\to\lambda_{\rm LQ}^{3i}\lambda_{\rm LQ}^{1i}\},$$

$$B_R^{\lambda_{\rm LQ}}(\tau\to \mu\gamma)=B_R^{\rm exp}(\tau^-\to\mu^-\overline{\nu}_\mu\nu_\tau)\times B_R^{\lambda_{\rm LQ}}(\mu\to e\gamma)\times\{\lambda_{\rm LQ}^{2i}\lambda_{\rm LQ}^{1i}\to\lambda_{\rm LQ}^{3i}\lambda_{\rm LQ}^{2i}\},\tag{6}$$

where the electron and muon masses have been neglected with respect to the τ mass. The central value of the experimental branching ratio for $\tau^-\to\mu^-\overline{\nu}_\mu\nu_\tau$ is $B_R^{\rm exp}(\tau^-\to\mu^-\overline{\nu}_\mu\nu_\tau)=17.37\%$ [24].

III. $\mu\to 3e$ DECAY AND μ-e CONVERSION IN NUCLEI

The most general lepton-family violating $(\Delta L=1)$ effective Hamiltonian which describes the amplitude of the $\mu\to 3e$ decay is

$$H^{(\Delta L=1)}=\frac{4G_F}{\sqrt{2}}\{Q_{LR}C_{LR}+Q_{RL}C_{RL}+C_1(\overline{e}_R\mu_L)(\overline{e}_Re_L)+C_2(\overline{e}_L\mu_R)(\overline{e}_Le_R)+C_3(\overline{e}_R\gamma_\mu\mu_R)(\overline{e}_R\gamma^\mu e_R)+C_4(\overline{e}_L\gamma_\mu\mu_L)(\overline{e}_L\gamma^\mu e_L)+C_5(\overline{e}_R\gamma_\mu\mu_R)\times(\overline{e}_L\gamma^\mu e_L)+C_6(\overline{e}_L\gamma_\mu\mu_L)(\overline{e}_R\gamma^\mu e_R)+\text{H.c.}\},\tag{7}$$

where Q_{LR} and Q_{RL} are the magnetic-dipole operators defined in Sec. II and the chiral fields are given by $\psi_{L,R}=1/2(1\mp\gamma_5)\psi$. In the LQ model obtained with the Lagrangian (2), the Wilson coefficients of the local four-fermion operators in (7) get their contributions from the photon-penguin, Z penguins, and the box diagrams [see Figs. 1(a)–1(c)] with $f=e$ and scalar and vectorial LQs running in the loops together with quarks).[3] In the limit of large LQ masses (large compared to the quark ones), the leading contribution to the effective Hamiltonian in (7) is given by the photon-penguin diagrams which affect only the coefficients C_3, C_4, C_5, and C_6. Indeed, in the large LQ mass limit, these diagrams are only ''mildly'' GIM suppressed since they are proportional to the $\lambda_{\rm LQ}^2\log(m_q^2/m_{\rm LQ}^2)/m_{\rm LQ}^2$; this, in the context of the GIM mechanism, is in contrast with the naive expectation of them being of order $O(\lambda_{\rm LQ}^2m_q^2/m_{\rm LQ}^4)$ and $O(\lambda_{\rm LQ}^4m_q^2/m_{\rm LQ}^4)$, which is typical of the Z penguins and box diagrams, respectively. We stress that the appearance of the $\log(m_q^2/m_{\rm LQ}^2)$ enhancements is a special property of the gamma-penguin diagrams which is independent by any assumption on the unitarity of the LQ couplings.

The relevance of these log enhancements in constraining the new physics beyond the SM was first analyzed in Ref. [15]. A more accurate discussion on the origin of these logarithms can be found in Ref. [16]. Here we want to point out that this mild GIM suppression of the photon-penguins, which is also present in the SM, is a peculiar property of the LQ interactions and it is not true in general extensions of the SM. For example, in the minimal supersymmetric SM, due to the super-GIM mechanism, the photon-penguins mediated by the charged Higgs, gauginos or Higgsinos are always GIM suppressed by terms of order $O(m_q^2/m_{\rm SUSY}^2)$ [with $m_{\rm SUSY}$ standing for any typical supersymmetric mass running in the loops] [23,25].

Therefore, due to these log enhancements, the $\mu\to 3e$ decay plays a crucial role in setting strong constraints on the FC LQs couplings in the $\Delta L=1$ processes. The branching ratio for this process is proportional to $\alpha^2/(m_{\rm LQ}^2G_F)^2\times\log(m_q/m_{\rm LQ})$, while the branching ratio of the $\mu\to e\gamma$ decay is proportional to $\alpha/(m_{\rm LQ}^2G_F)^2\times(m_q/m_{\rm LQ})^4$. Therefore even though in the branching ratio of the $\mu\to 3e$ decay we pay the price of an extra electromagnetic α coupling, with respect to the $\mu\to e\gamma$, in the large LQ mass limit the α

[3]In the case of unitary couplings any single diagram of the gamma- or Z-penguin type is finite. This is because the divergent part, being flavor independent, factorizes out in sum $\Sigma_i\lambda_{\rm LQ}^{\dagger mi}\lambda_{\rm LQ}^{in}$ on the internal-flavor index i=1,2,3... and therefore its contribution vanishes for $m\neq n$. In the case of nonunitary couplings, due to the $U(1)\times SU(2)_L$ Ward identities, only the total sum of the gamma-penguin-diagrams, or analogously the Z-penguin ones (including also the diagrams with the self-energy insertions), are finite. On the contrary the magnetic-penguin- and box-diagrams [see Figs. 1(c)–1(d)], respectively] are just finite since their loop integrals are convergent. Clearly, in the vectorial sector, the above arguments hold if the vectorial LQs are of the gauge type and acquire mass via spontaneous symmetry breaking.

suppression could dominate the $m_q^4/m_{\rm LQ}^4$ term. For this reason we neglect the effects of the magnetic-penguins operators Q_{LR} and Q_{RL} in the $\mu\to 3e$ branching ratio.[4] The main contribution to the branching ratio of $\mu\to 3e$ is given by [26]

$$B_R=2\left(\frac{|C_1|^2}{16}+\frac{|C_2|^2}{16}+|C_3|^2+|C_4|^2\right)+|C_5|^2+|C_6|^2, \tag{8}$$

where C_i are defined in Eq. (7). Note that the terms suppressed by m_e/m_μ have been neglected. In addition in obtaining Eq. (8) the total width of the muon was approximated and we used instead the width of the main decay $\mu^-\to\nu_\mu e^-\overline{\nu_e}$ whose branching ratio is almost 100%. Moreover, by following the approach adopted in this analysis, we consider the photon-penguin's contributions induced by only one LQ couplings and by ''switching off'' all the others. By means of these approximations and by neglecting the terms proportional to the quark masses, the expression for the branching ratio in Eq. (8) can be further simplified, since in this case we have $C_{1,2}=0$, $C_3=C_5$ and $C_4=C_6$. We next give the analytical results relative to the branching ratio of $\mu\to 3e$ mediated by the photon-penguins (the analogous results in the τ sector can be obtained by means of a simple generalization).

Gauge-vectorial LQs:

$$B_R^{\lambda_{LV_0}}=\frac{\tilde{B}_V}{m_{V_0}^4 G_F^2}Q_D^2\left[\sum_{i=1}^{3}\lambda_{LV_0}^{2i}\lambda_{LV_0}^{1i}\log\left(\frac{m_{D_i}^2}{m_{V_0}^2}\right)\right]^2,$$

$$B_R^{\lambda_{RV_0}}=B_R^{\lambda_{LV_0}}(\lambda_{LV_0}\to\lambda_{RV_0}),$$

$$B_R^{\lambda_{R\tilde{V}_0}}=\frac{\tilde{B}_V}{m_{\tilde{V}_0^2}^4 G_F^2}Q_U^2\left[\sum_{i=1}^{3}\lambda_{R\tilde{V}_0}^{2i}\lambda_{R\tilde{V}_0}^{1i}\log\left(\frac{m_{U_i}^2}{m_{\tilde{V}_0}^2}\right)\right.$$
$$\left.\times(1+\delta_{i3}\Delta_V(x_t,R_{\tilde{V}_0}))\right]^2,$$

$$B_R^{\lambda_{LV_{1/2}}}=\frac{\tilde{B}_V}{m_{V_{1/2}}^4 G_F^2}Q_D^2\left[\sum_{i=1}^{3}\lambda_{LV_{1/2}}^{2i}\lambda_{LV_{1/2}}^{1i}\log\left(\frac{m_{D_i}^2}{m_{V_{1/2}}^2}\right)\right]^2,$$

$$B_R^{\lambda_{RV_{1/2}}}=\frac{\tilde{B}_V}{m_{V_{1/2}}^4 G_F^2}\left[\sum_{i=1}^{3}\lambda_{RV_{1/2}}^{2i}\lambda_{RV_{1/2}}^{1i}\left(Q_D\log\left(\frac{m_{D_i}^2}{m_{V_{1/2}}^2}\right)\right.\right.$$
$$\left.\left.+Q_U\log\left(\frac{m_{U_i}^2}{m_{V_{1/2}}^2}\right)(1+\delta_{i3}\Delta_V(x_t,-R_{V_{1/2}^U}))\right)\right]^2,$$

$$B_R^{\lambda_{L\tilde{V}_{1/2}}}=\frac{\tilde{B}_V}{m_{\tilde{V}_{1/2}}^4 G_F^2}Q_U^2\left[\sum_{i=1}^{3}\lambda_{L\tilde{V}_{1/2}}^{2i}\lambda_{L\tilde{V}_{1/2}}^{1i}\log\left(\frac{m_{U_i}^2}{m_{\tilde{V}_{1/2}}^2}\right)\right.$$
$$\left.\times(1+\delta_{i3}\Delta_V(x_t,-R_{\tilde{V}_{1/2}^D}))\right]^2,$$

$$B_R^{\lambda_{LV_1}}=\frac{\tilde{B}_V}{m_{V_1}^4 G_F^2}\left[\sum_{i=1}^{3}\lambda_{LV_1}^{2i}\lambda_{LV_1}^{1i}\left(Q_D\log\left(\frac{m_{D_i}^2}{m_{V_1}^2}\right)\right.\right.$$
$$\left.\left.+2Q_U\log\left(\frac{m_{U_i}^2}{m_{V_1}^2}\right)(1+\delta_{i3}\Delta_V(x_t,R_{V_1}))\right)\right]^2. \tag{9}$$

Scalar LQs:

$$B_R^{\lambda_{LS_0}}=\frac{\tilde{B}_S}{m_{S_0}^4 G_F^2}Q_U^2\left[\sum_{i=1}^{3}\lambda_{LS_0}^{2i}\lambda_{LS_0}^{1i}\log\left(\frac{m_{U_i}^2}{m_{S_0}^2}\right)\right.$$
$$\left.\times(1+\delta_{i3}\Delta_S(x_t,-R_{S_0}))\right]^2,$$

$$B_R^{\lambda_{RS_0}}=B_R^{\lambda_{LS_0}}(\lambda_{LS_0}\to\lambda_{RS_0}),$$

$$B_R^{\lambda_{R\tilde{S}_0}}=\frac{\tilde{B}_S}{m_{\tilde{S}_0^2}^4 G_F^2}Q_D^2\left[\sum_{i=1}^{3}\lambda_{R\tilde{S}_0}^{2i}\lambda_{R\tilde{S}_0}^{1i}\log\left(\frac{m_{D_i}^2}{m_{\tilde{S}_0}^2}\right)\right]^2,$$

$$B_R^{\lambda_{LS_{1/2}}}=\frac{\tilde{B}_S}{m_{S_{1/2}}^4 G_F^2}Q_U^2\left[\sum_{i=1}^{3}\lambda_{LS_{1/2}}^{2i}\lambda_{LS_{1/2}}^{1i}\log\left(\frac{m_{U_i}^2}{m_{S_{1/2}}^2}\right)\right.$$
$$\left.\times(1+\delta_{i3}\Delta_S(x_t,R_{S_{1/2}^D}))\right]^2,$$

$$B_R^{\lambda_{RS_{1/2}}}=\frac{\tilde{B}_S}{m_{S_{1/2}}^4 G_F^2}\left[\sum_{i=1}^{3}\lambda_{RS_{1/2}}^{2i}\lambda_{RS_{1/2}}^{1i}\left(Q_D\log\left(\frac{m_{D_i}^2}{m_{S_{1/2}}^2}\right)\right.\right.$$
$$\left.\left.+Q_U\log\left(\frac{m_{U_i}^2}{m_{S_{1/2}}^2}\right)(1+\delta_{i3}\Delta_S(x_t,R_{S_{1/2}^D}))\right)\right]^2,$$

[4]We recall that if the Wilson coefficients of the magnetic-penguin operators in (7) are not suppressed then their contribution can give sizable effects to the $\mu\to 3e$ decay [26]. Moreover, after the phase space integration, some terms (proportional to the magnetic-penguin contributions) get an enhancement of $\log(m_\mu/m_e)$ in the decay rate because of the $1/q^2$ pole of the gamma propagator. Therefore, if these diagrams are included then the approximation consisting of the neglect of the electron mass, cannot be used.

$$B_R^{\lambda_{L\tilde{S}_{1/2}}}=\frac{\tilde{B}_S}{m_{\tilde{S}_{1/2}}^4 G_F^2}Q_D^2\left[\sum_{i=1}^{3}\lambda_{L\tilde{S}_{1/2}}^{2i}\lambda_{L\tilde{S}_{1/2}}^{1i}\log\left(\frac{m_{D_i}^2}{m_{\tilde{S}_{1/2}}^2}\right)\right]^2,$$

$$B_R^{\lambda_{LS_1}}=\frac{\tilde{B}_S}{m_{S_1}^4 G_F^2}\left[\sum_{i=1}^{3}\lambda_{LS_1}^{2i}\lambda_{LS_1}^{1i}\left(Q_U\log\left(\frac{m_{U_i}^2}{m_{S_1}^2}\right)\times(1+\delta_{i3}\Delta_S(x_t,-R_{S_3}))+2Q_D\log\left(\frac{m_{D_i}^2}{m_{S_1}^2}\right)\right)\right]^2, \tag{10}$$

where $\tilde{B}_V=\alpha^2N_c^2/(96\pi^2)$ and $\tilde{B}_S=\alpha^2N_c^2/(384\pi^2)$. The functions $\Delta_{S,V}(x_t,R_{\rm LQ})$ (where δ_{ij} is the standard delta function, $x_t=m_t^2/m_{\rm LQ}^2$ and $R_{\rm LQ}\equiv Q_{LQ}/Q_U$) whose expressions are given in the Appendix, take into account the exact dependence on the top mass m_t. Note that in the limit $\lim_{x_t\to 0}(\Delta_{S,V}(x_t,R_{LQ}))\to 0$. The results in Eqs. (9), (10) are in agreement with the analogous ones obtained in Refs. [23,25] for the supersymmetric corrections to the FCNC processes in the quark sector.

In the τ sector the corresponding analytical results for the $\tau\to 3e$ and $\tau\to 3\mu$ decays are obtained by making the following substitutions in the r.h.s. of Eqs. (9), (10),

$$B_R^{\lambda_{\rm LQ}}(\tau\to 3e)=B_R^{\rm exp}(\tau^-\to\mu^-\overline{\nu}_\mu\nu_\tau)\times B_R^{\lambda_{\rm LQ}}(\mu\to 3e)\times\{\lambda_{\rm LQ}^{2i}\lambda_{\rm LQ}^{1i}\to\lambda_{\rm LQ}^{3i}\lambda_{\rm LQ}^{1i}\},$$

$$B_R^{\lambda_{\rm LQ}}(\tau\to 3\mu)=B_R^{\rm exp}(\tau^-\to\mu^-\overline{\nu}_\mu\nu_\tau)\times B_R^{\lambda_{\rm LQ}}(\mu\to 3e)\times\{\lambda_{\rm LQ}^{2i}\lambda_{\rm LQ}^{1i}\to\lambda_{\rm LQ}^{3i}\lambda_{\rm LQ}^{2i}\}. \tag{11}$$

We now consider the LQ contribution to the $\mu-e$ conversion in nuclei [17–22]. The most general effective Hamiltonian which is relevant for this process is given by

$$\begin{aligned}H_{\rm hadr}^{(\Delta L=1)}=\frac{4G_F}{\sqrt{2}}\{&Q_{LR}C_{LR}+Q_{RL}C_{RL}\}+C_1^h(\overline{e_R}\mu_L)\sum_{q=u,d}(\overline{q_R}q_L)+C_2^h(\overline{e_L}\mu_R)\sum_{q=u,d}(\overline{q_L}q_R)+C_3^h(\overline{e_L}\mu_R)\sum_{q=u,d}(\overline{q_L}q_R)\\&+C_4^h(\overline{e_L}\mu_R)\sum_{q=u,d}(\overline{q_L}q_R)+C_5^h(\overline{e_R}\gamma_\mu\mu_R)\sum_{q=u,d}Q_q(\overline{q_R}\gamma^\mu q_R)+C_6^h(\overline{e_L}\gamma_\mu\mu_L)\sum_{q=u,d}Q_q(\overline{q_L}\gamma^\mu q_L)\\&+C_7^h(\overline{e_R}\gamma_\mu\mu_R)\sum_{q=u,d}Q_q(\overline{q_L}\gamma^\mu q_L)+C_8^h(\overline{e_L}\gamma_\mu\mu_L)\sum_{q=u,d}Q_q(\overline{q_R}\gamma^\mu q_R)+\text{H.c.},\end{aligned} \tag{12}$$

where in the quark q fields the sum over color indices is assumed and Q_q is the quark electric charge in the unit of e. Note that for the Wilson coefficients C_i^h we have used a normalization which is different from the one used in (7). In the LQ model the Wilson coefficients of the four-fermion operators get their contribution at tree-level with a LQ exchange. The tree-level contributions involve only the products of the LQ couplings $\lambda_{\rm LQ}^{21}\lambda_{\rm LQ}^{11}$, since the operators in (12) contain only quarks of the first generation. Indeed this process is known to be particularly effective for setting strong bounds on this combination of couplings [8,10]. However the Wilson coefficients C_i^h also receive the next-to-leading contributions from the one-loop diagrams induced by the photon-penguins, Z-penguins, and box diagrams [see Figs. 1(a)–1(c) with $f=U,D$ quarks]. These next-to-leading contributions involve the products of the $\lambda_{\rm LQ}^{2i}\lambda_{\rm LQ}^{1i}$ combinations with $i=1,2,3$; as a result the $\mu-e$ conversion process can also give the possibility to set constraints on the second and third quark generations.[5] In particular, in order to set bounds from the $\mu-e$ conversion on the combinations $\lambda_{\rm LQ}^{2i}\lambda_{\rm LQ}^{1i}/m_{\rm LQ}^2$ with $i=2,3$, we assume that its branching ratio is dominated by the one-loop contributions. This implies that the product $\lambda_{\rm LQ}^{21}\lambda_{\rm LQ}^{11}$ should be negligible with respect to the products $\lambda_{\rm LQ}^{2i}\lambda_{\rm LQ}^{1i}$ (with $i=2,3$) times electromagnetic constant α. This condition does not violate the unitarity of the $\lambda_{\rm LQ}$ matrices since in this case one can still have $\lambda_{\rm LQ}^{22}\lambda_{\rm LQ}^{12}=-\lambda_{\rm LQ}^{23}\lambda_{\rm LQ}^{13}+O(\lambda_{\rm LQ}^{21}\lambda_{\rm LQ}^{11})$. Now, even though the constraints on couplings involving the second and third quark generations are weaker than the corresponding ones with the first generation, they should be compared to the same bounds obtained by other processes, such as for example the $\mu\to 3e$ decay. Indeed, as we will show in the next section, the bounds on the LQ couplings involving the second and third quark generations, which we obtained from the current experimental upper limit on the $\mu-e$ conversion rate, are stronger than the corresponding ones obtained from the $\mu\to 3e$ decay.

In the large LQ mass limit, the photon-penguin diagrams, due to the log enhancements, dominate the other one-loop

[5]In a more recent paper the authors of Ref. [22] stress the importance of the log enhancements, induced in the μ-e conversion rate by the photon penguins, in constraining the supersymmetric R-parity violating models. However in these models the tree-level contributions to the μ-e conversion are absent.

diagrams, such as the Z-penguins and box diagrams which are of order $O(m_q^2/m_{\rm LQ}^2)$. Therefore in constraining the LQ couplings involving the second and third quark generations we assume that the μ-e conversion is dominated by the photon-conversion mechanism [17–21]. In this case only the matrix elements of the hadronic electromagnetic current between nuclei are involved. In order to calculate the nuclear form factors connected to the electromagnetic matrix elements, various models and approximations have been applied in literature [17–21]. In Ref. [18], and more recently in Ref. [19], the relativistic effects have been taken into account. However, due to the large mass of the muon, it is useful to take the nonrelativistic limit of the motion of the muon in the muonic atom (see Ref. [20] and more recently Ref. [21]). Indeed, in this limit, the large uncertainty connected to the muon wave function factorizes out in the calculation of the coherent conversion rate. In order to estimate the LQ contribution to the $\mu-e$ conversion in nuclei N [defined as $B_R(\mu-e)_N \equiv \Gamma(\mu N\to eN)/\Gamma(\mu N\to \nu_\mu N')$], we use the nonrelativistic results of Ref. [20]. In the photon-conversion mechanism one can set $C_i^h=0$, $\quad i=1,\ldots,4$, $C_5^h = C_7^h$, and $C_6^h=C_8^h$ in the Hamiltonian (12), and the branching ratio is given by [20,22]

$$B_R(\mu-e)_N = C\,\frac{\alpha^3 m_\mu^5 Z_{\rm eff}^4 Z|\overline{F}_p|^2}{\Gamma_{\rm capt}}\,\frac{1}{4\pi^2}(|C_5^h|^2+|C_8^h|^2), \qquad (13)$$

where $\overline{F}_p(q)$ is the proton nuclear form factor (see Ref. [20] for more details) and $\Gamma_{\rm capt}$ is the total muon capture rate.[6] All these quantities depend upon the titanium element ($^{48}_{22}$Ti) used in the current experiment [27]. For the Ti the quantities appearing in Eq. (13) take the following values [20]: $C^{\rm Ti}=1.0$, $Z_{\rm eff}^{\rm Ti}=17.61$, $Z^{\rm Ti}=22$, $\Gamma_{\rm capt}^{\rm Ti}=2.59\times 10^6\ {\rm s}^{-1}$, and $\overline{F}_p^{\rm Ti}(q)=0.55$.

By taking into account only the photon-penguin contributions we see that, respectively, the C_5^h and C_6^h coefficients are proportional to C_3 and C_6 in Eq. (7) by an overall factor. This factor is a constant and does not depend upon the particular LQ model considered. This implies that the LQ contributions to the branching ratio of the μ-e conversion in nuclei, mediated by the photon-conversion mechanism, have the same expression of Eqs. (9), (10) and so the bounds extracted from this process can be simply obtained by rescaling the relative bounds obtained from the $\mu\to 3e$ decay. In order to obtain the corresponding analytical expressions of Eqs. (9), (10) for the branching ratios of the μ-e photon-conversion in nuclei, the following substitution has to be made in the r.h.s of Eqs. (9), (10):

$$B_R^{\lambda_{\rm LQ}}(\mu-e)_{\rm Ti} = B_R^{\lambda_{\rm LQ}}(\mu\to 3e)\left\{\frac{1}{G_F^2}\right.$$
$$\left.\to C\,\frac{\alpha^3 m_\mu^5 Z_{\rm eff}^4 Z|\overline{F}_p|^2}{\Gamma_{\rm capt}}\,\frac{2}{3\pi^2}\right\}, \qquad (14)$$

where, as in the $\mu\to 3e$ case, we make active the effect of one single coupling $\lambda_{\rm LQ}$ per time by ‘‘switching off’’ all the others.

IV. NUMERICAL RESULTS FOR THE BOUNDS

In this section we present the numerical results for the bounds on the combinations of LQ couplings $\lambda_{\rm LQ}^{ij}$ and masses $m_{\rm LQ}$ obtained from the $\mu\to 3e$, μ-e conversion in Ti, and the $\mu\to e\gamma$. In addition we give the results for the corresponding bounds in the τ sector. In setting constraints on the product of couplings $\lambda_{\rm LQ}^{2i}\lambda_{\rm LQ}^{1i}$ $(i=1,2,3)$, in order to simplify our study, we use the following approach.

The tree-level LQ’s contribution to the $\mu-e$ conversion rate (not mediated by the photon-conversion mechanism) contains only the terms $\lambda_{\rm LQ}^{21}\lambda_{\rm LQ}^{11}$. This process is used to strongly constrain the combinations $|\lambda_{\rm LQ}^{21}\lambda_{\rm LQ}^{11}/m_{\rm LQ}^2|$.

In order to set bounds on the LQ couplings involving the second and third generations of quarks, we adopt the approximation which neglects $\lambda_{\rm LQ}^{21}\lambda_{\rm LQ}^{11}$ with respect to $\lambda_{\rm LQ}^{22}\lambda_{\rm LQ}^{12}$ and $\lambda_{\rm LQ}^{23}\lambda_{\rm LQ}^{13}$ in the one-loop contributions. This approximation can be justified as follows. The products of couplings $\lambda_{\rm LQ}^{2i}\lambda_{\rm LQ}^{1i}$, $i=2,3$ enter only in the one-loop contribution to the $\mu\to e\gamma$, $\mu\to 3e$ decays, and the $\mu-e$ conversion. Therefore they could be larger if compared with the $\lambda_{\rm LQ}^{21}\lambda_{\rm LQ}^{11}$ ones without violating the experimental upper limits on the branching ratios.

In this approximation the unitarity of the $\lambda_{\rm LQ}$ matrices implies that: $\lambda_{\rm LQ}^{22}\lambda_{\rm LQ}^{12}=-\lambda_{\rm LQ}^{23}\lambda_{\rm LQ}^{13}$. This condition allows us to eliminate one of the two products of couplings in the one-loop contributions and set bounds for the magnitude of the combinations $|\lambda_{\rm LQ}^{22}\lambda_{\rm LQ}^{12}|/m_{\rm LQ}^2$ or $|\lambda_{\rm LQ}^{23}\lambda_{\rm LQ}^{13}|/m_{\rm LQ}^2$ by means of Eqs. (4), (5), (9), (10). In order to set bounds in the sector i, with $i=2,3$, by means of the $\mu-e$ conversion one assumes that (for this process) the photon-conversion mechanism dominates over the nonphotonic one.

The same approach is adopted in setting bounds in the τ sector. The relevant effective Hamiltonians for the $\tau\to\pi^0 e$ and $\tau\to\pi^0\mu$ decays are induced at the tree-level and so these processes are used to strongly constrain the variables $|\lambda_{\rm LQ}^{31}\lambda_{\rm LQ}^{11}|/m_{\rm LQ}^2$ and $|\lambda_{\rm LQ}^{31}\lambda_{\rm LQ}^{21}|/m_{\rm LQ}^2$, respectively. The terms $\lambda_{\rm LQ}^{3i}\lambda_{\rm LQ}^{1i}$ and $\lambda_{\rm LQ}^{3i}\lambda_{\rm LQ}^{2i}$ (involving the second and third quark generations) enter at one-loop level and therefore, as in the muon sector, we assume that they could be larger than the corresponding ones involving the first generation. The bounds on these combinations of couplings are obtained by imposing the experimental upper limits on the $\tau\to e\gamma$, $\tau\to 3e$, $\tau\to\mu\gamma$, and $\tau\to 3\mu$ decays.

[6]Note that with respect to the corresponding formula of Ref. [22], we have simplified the $1/q^2$ pole of the photon propagator (which for this process is of order $|q^2|\simeq m_\mu^2$) with the q^2 which, due to the gauge-invariance, factorizes in the photon-penguin form factor.

TABLE II. Numerical upper bounds for the vectorial and scalar $SU(2)_L$-*singlet*-LQ variables $\xi^i_{\rm LQ}\equiv|\lambda^{2i}_{\rm LQ}\lambda^{1i}_{\rm LQ}|\times(10^2\ {\rm GeV}/m_{\rm LQ})^2<(\xi^i_{\rm LQ})^B$ obtained from the experimental upper limits on the $(\mu-e)_{Ti}$ conversion rate and $\mu\to 3e$ decay. In the $\mu\to e\gamma$ rows the variables which are constrained are $\tilde{\xi}^i_{\rm LQ}\equiv\sqrt{|\lambda^{2i}_{\rm LQ}\lambda^{1i}_{\rm LQ}|}\times(10^2\ {\rm GeV}/m_{\rm LQ})^2<(\xi^i_{\rm LQ})^B$. Note that the symbol $--$ stands for weaker constraints, see the text. Everywhere $(\xi^2_{\rm LQ})^B=(\xi^3_{\rm LQ})^B$.

Vector	i	$(\xi^i_{LV_0})^B$	$(\xi^i_{RV_0})^B$	$(\xi^i_{R\tilde{V}_0})^B$
$(\mu-e)_{Ti}$	1	2.6×10^{-7}	2.6×10^{-7}	2.6×10^{-7}
$(\mu-e)_{Ti}$	2,3	1.5×10^{-5}	1.5×10^{-5}	4.6×10^{-6}
$\mu\to 3e$	2,3	8.0×10^{-5}	8.0×10^{-5}	2.5×10^{-5}
$\mu\to e\gamma$	2,3	$--$	$--$	1.7×10^{-3}
Scalar	i	$(\xi^i_{LS_0})^B$	$(\xi^i_{RS_0})^B$	$(\xi^i_{R\tilde{S}_0})^B$
$(\mu-e)_{Ti}$	1	5.2×10^{-7}	5.2×10^{-7}	5.2×10^{-7}
$(\mu-e)_{Ti}$	2,3	9.2×10^{-6}	9.2×10^{-6}	3.0×10^{-5}
$\mu\to 3e$	2,3	5.0×10^{-5}	5.0×10^{-5}	1.6×10^{-4}
$\mu\to e\gamma$	2,3	2.3×10^{-3}	2.3×10^{-3}	4.5×10^{-2}

In Tables II and III we present our results for the upper bounds on the following variables $\xi^i_{\rm LQ}\equiv|\lambda^{2i}_{\rm LQ}\lambda^{1i}_{\rm LQ}|\times(10^2\ {\rm GeV}/m_{\rm LQ})^2$ and $\tilde{\xi}^i_{\rm LQ}\equiv\sqrt{|\lambda^{2i}_{\rm LQ}\lambda^{1i}_{\rm LQ}|}\times(10^2\ {\rm GeV}/m_{\rm LQ})^2$ with $i=1,2,3$. The constraints on $\xi^1_{\rm LQ}$ are obtained by using the same approach used in Ref. [10]. In addition, by means of the current experimental upper limits on the $\mu-e$ conversion rate on Ti which is $B^{\rm exp}_R(\mu-e)_{Ti}<6.1\times10^{-13}$ [27], we improve the results of Ref. [10]. From Tables II, III we see that the current limits on the $\mu-e$ conversion rate can set bounds on $\xi^1_{\rm LQ}$ which are at the level of $\xi^1_{\rm LQ}<O(10^{-7})$. Our results for the bounds on $\xi^1_{\rm LQ}$ are in agreement with the corresponding ones in Ref. [10] except for $\xi^1_{RV_{1/2}}$ and $\xi^1_{RS_{1/2}}$: in these cases we have an analytical factor 2 of discrepancy with [10]. (In particular our expressions for the bounds on $\xi^1_{RV_{1/2}}$ and $\xi^1_{RS_{1/2}}$ are half of the corresponding ones in [10].) However, our results are consistent

TABLE III. Numerical bounds as in Table II which here are relative to the $SU(2)_L$-*doublet*- and $SU(2)_L$-*vector*-LQs.

Vector	i	$(\xi^i_{LV_{1/2}})^B$	$(\xi^i_{RV_{1/2}})^B$	$(\xi^i_{L\tilde{V}_{1/2}})^B$	$(\xi^i_{LV_1})^B$
$(\mu-e)_{Ti}$	1	2.6×10^{-7}	1.3×10^{-7}	2.6×10^{-7}	8.5×10^{-8}
$(\mu-e)_{Ti}$	2,3	1.5×10^{-5}	6.7×10^{-6}	4.6×10^{-6}	2.7×10^{-6}
$\mu\to 3e$	2,3	8.0×10^{-5}	3.7×10^{-5}	2.5×10^{-5}	1.5×10^{-5}
$\mu\to e\gamma$	2,3	8.4×10^{-2}	2.9×10^{-3}	2.9×10^{-3}	1.2×10^{-3}
Scalar	i	$(\xi^i_{LS_{1/2}})^B$	$(\xi^i_{RS_{1/2}})^B$	$(\xi^i_{L\tilde{S}_{1/2}})^B$	$(\xi^i_{LS_1})^B$
$(\mu-e)_{Ti}$	1	5.2×10^{-7}	2.6×10^{-7}	5.2×10^{-7}	1.7×10^{-7}
$(\mu-e)_{Ti}$	2,3	9.2×10^{-6}	1.3×10^{-5}	3.0×10^{-5}	2.5×10^{-5}
$\mu\to 3e$	2,3	5.0×10^{-5}	7.3×10^{-5}	1.6×10^{-4}	1.3×10^{-4}
$\mu\to e\gamma$	2,3	1.7×10^{-3}	1.7×10^{-3}	5.1×10^{-2}	2.3×10^{-3}

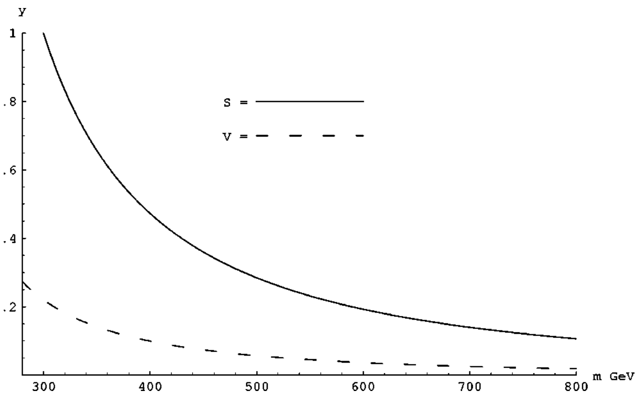

FIG. 2. Plots for $y=|\Delta_S(x_t,Q)|$ (continuous) and $y=|\Delta_V(x_t,Q)|$ (dashed) functions, with $x_t=m_t^2/m^2_{\rm LQ}$ and $Q=-5/2$, versus $m=m_{\rm LQ}$ in GeV.

with the effective Hamiltonian and the approximation[7] used in [10] for calculating the hadronic matrix elements.

Now we analyze the results in Tables II and III for the upper bounds[8] on $\xi^{i=2,3}_{LQ}$ which come from the $\mu\to 3e$ decay where the current experimental upper limit on the branching ratio is $B^{\rm exp}_R(\mu\to 3e)<10^{-12}$ at 90% C.L. [24]. These bounds are obtained in the approximation of large LQ mass limit and so by setting to zero the $\Delta_{V,S}$ functions in (9), (10) which are of order $O(m_t^2/m^2_{\rm LQ})$. Moreover the following values of the quark masses are used: $m_s=150$ MeV, $m_c=1.5$ GeV, $m_b=5$ GeV, and $m_t=175$ GeV; these correspond to the central values of the allowed ranges [24]. From these results we see that the current upper limits on $\mu\to 3e$ can set bounds on $\xi^{2,3}_{\rm LQ}$ which are at the level of $\xi^{2,3}_{\rm LQ}<O(10^{-5}-10^{-4})$. These constraints are consistent with the main approximation used in our analysis which neglects $\xi^1_{\rm LQ}$ with respect to $\xi^{(2,3)}_{\rm LQ}$. Note that, due to the unitarity of the $\lambda_{\rm LQ}$ matrices, the logarithmic dependence of the LQ mass in the right-hand side of Eqs. (9), (10) disappears and it is replaced by the logarithmic dependence of the corresponding quark masses ratio $\log(m_{q_2}/m_{q_3})$ involving only the second and third generation. Therefore, due to the logarithmic dependence upon the quark masses in Eqs. (9), (10), the uncertainties which affect the bounds on $\xi^{i=2,3}_{\rm LQ}$ (from $\mu\to 3e$), induced by the uncertainties on the quark masses, are small and are of order $O(10\%)$.

In order to estimate the reliability of the leading logarithmic approximation when the top mass is involved, we plot (see Figs. 2 and 3) the absolute values of the functions $\Delta_{V,S}(x_t,Q)$ versus the LQ mass $m_{\rm LQ}$. These plots have origin in $m_{\rm LQ}=280$ GeV which roughly corresponds to the exclusion limit obtained at HERA [14] for LQ masses with couplings of electromagnetic strength. From Figs. 2, 3 one can conclude that these corrections are smaller than 20% for

[7]This approximation mainly consists in assuming that the matrix elements, corresponding to the amplitudes μ Ti$\to e$ Ti and μ Ti $\to\nu_\mu$ Ti$'$, are comparable.

[8]Note that, in our approach, the bounds on $\xi^{i=2}_{\rm LQ}$ and $\xi^{i=3}_{\rm LQ}$ turn out to be the same.

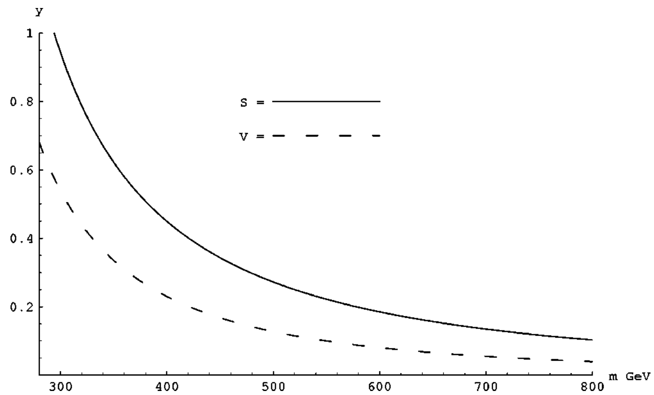

FIG. 3. The same plots as in Fig. 2 but for $Q=1/2$.

moderate values of the LQ masses, in particular (scalar) $m_S > 600$ GeV and (vectorial) $m_V > 400$ GeV. For the intermediate LQ mass regions, the corrections induced by the Z-penguin and box diagrams, which are of order $O(m_t^2/m_{\rm LQ}^2)$, become relevant and they should be included in the analysis. In these cases one cannot constrain a single variable combination as the $\xi_{\rm LQ}^i$ and this results in a complication of the analysis. However the excluded regions in the $m_{\rm LQ}$ and $\lambda_{\rm LQ}^{1i}\lambda_{\rm LQ}^{2i}$ plane could be analyzed, for example, by means of contour plots. A complete study for this scenario will be presented elsewhere [28].

The bounds on $\xi_{\rm LQ}^{i=2,3}$, which come from the $\mu-e$ photon-conversion, are simply obtained by rescaling the corresponding results of $\mu\to 3e$ in Tables II, III by a constant factor. Clearly this factor depends upon the experimental upper limits on the $\mu-e$ conversion and $\mu\to 3e$ branching ratios. In particular, by inserting (14) into (9) and (10), we get the following results for the bounds:

$$(\xi_{\rm LQ}^i)_{\rm Ti}^{\mu-e} \simeq \frac{1}{5.4}(\xi_{\rm LQ}^i)^{\mu\to 3e}. \tag{15}$$

However we stress that, even though the $\mu\to 3e$ process can set (at present) weaker constraints than the $(\mu-e)_{Ti}$ conversion, the latter is model dependent (due to the determination of the nuclear wave functions and form factors) while the former is not.

In Tables II, III for comparison we also give the bounds obtained from the negative searches of the $\mu\to e\gamma$ decay where the current experimental upper limit on the branching ratio is ${\rm Br}(\mu\to e\gamma) < 1.2\times 10^{-11}$ at 90% C.L. [29]. Due to the higher inverse-powers in LQ-mass dependence in Eqs. (4), (5), it appears natural to constrain the variables $\tilde{\xi}_{\rm LQ}^i$. From Tables II, III we see that the bounds on $\tilde{\xi}_{\rm LQ}^i$ with $i=2,3$ are at the level of $\tilde{\xi}_{\rm LQ}^i < O(10^{-3}-10^{-2})$. In obtaining these results the terms proportional to the b quark mass with respect to the top ones have been neglected. Moreover in the case of the scalar LQs, in order to simplify the analysis, we replaced the function $\rho(x)$ in Eq. (5) by its average over the range $600 < m_{\rm LQ} < 2000$ GeV. For some bounds in the $\mu\to e\gamma$ rows, in particular $\tilde{\xi}_{LV_0}^{2,3}$ and $\tilde{\xi}_{RV_0}^{2,3}$, we have not shown the results (this is indicated by the symbol $--$ appearing in Tables II, III). The reason for not giving these bounds is that, at the amplitude level, there is an accidental cancellation of the leading term in the m_q^2/m_{LQ}^2 expansion [see Eq. (4)]. Therefore, due to a stronger GIM suppression of the next-to-leading contribution, we expect, in these cases, weaker bounds on masses and couplings combinations.

For fixed values of the LQ mass we can compare the bounds on the product of couplings $\lambda_{\rm LQ}^{2i}\lambda_{\rm LQ}^{1i}$ which come from the $\mu\to e\gamma$ and $\mu\to 3e$ decay (or $\mu-e$ conversion). In particular, from the results in Tables II, III, one can draw the following conclusions: for a LQ mass $m_{\rm LQ}\simeq 1$ TeV the bounds on the $\lambda_{\rm LQ}^{2i}\lambda_{\rm LQ}^{1i}$ combinations from $\mu\to 3e$ are stronger, of roughly one order of magnitude, than the corresponding best ones from the $\mu\to e\gamma$ decay. On the contrary, if we fix the couplings $\lambda_{\rm LQ}^{2,3}$ to be of the order of the electromagnetic strength, the bounds on the LQ masses induced by the $\mu\to 3e$ are at the level of $m_{\rm LQ} > (2-8)$TeV while the same constraints from $\mu\to e\gamma$ are $m_{\rm LQ} > 200$ GeV–1.3 TeV. In this respect one can argue that the bounds obtained from $\mu\to e\gamma$ are weaker than in $\mu\to 3e$ or $(\mu-e)_{Ti}$. Clearly the difference between these constraints becomes more noticeable in line with the increase of the LQ masses.

Now we compare the results in Tables II, III with the corresponding best bounds on $\xi_{\rm LQ}^i$ obtained by other processes. From the analysis of Ref. [10] we learn that the hadron-lepton universality and the ratio $R=\Gamma(\pi^+\to \bar{e}\nu)/\Gamma(\pi^+\to\bar{\mu}\nu)$ can set severe constraints on the $\lambda_{\rm LQ}^{21}\lambda_{\rm LQ}^{11}/m_{\rm LQ}^2$ variables involving the first quark generation. This is because the LQs contribute at tree-level to the neutron β decay, as well as to the $\pi^+\to\bar{e}\nu$ and $\pi^+\to\bar{\mu}\nu$, but only via box diagrams at $\mu\to e\bar{\nu}\nu$. Then the bounds coming from the hadron-lepton universality are obtained by requiring that the Fermi constant in the neutron β decay does not differ significantly from the muon decay measurement. These bounds are much weaker than the corresponding ones set by the $\mu-e$ conversion, roughly between three and four orders of magnitude weaker. Analogous conclusions hold for the bounds coming from the ratio R. However the R measurement is particularly effective in constraining the product of couplings with different chiralities (this special case is not considered in our analysis since it involves the product of two different couplings) at the level of $\lambda_{\rm Left}^{21}\lambda_{\rm Right}^{11} < 10^{-6}(m_{\rm LQ}/(100\ {\rm GeV}))^2$ [10].

In the K and π meson sector, there are no processes, induced by tree-level LQ exchanges, which could strongly constrain the $\lambda_{\rm LQ}^{22}\lambda_{\rm LQ}^{12}$ products [10]. This is not true anymore in the η meson sector. Indeed the $\eta\to\mu e$ decay, due to the $\bar{s}s$ quark's content of η, gets a tree-level LQ contribution containing the $\lambda_{\rm LQ}^{22}\lambda_{\rm LQ}^{12}$ product. However, we estimated that the bounds on $\xi_{\rm LQ}^2$ obtained by means of the experimental upper limit on the $\eta\to\mu e$ branching ratio [which is of order $O(10^{-6})$ [24]] are of order $O(1)$ in the same unity of Tables II, III. So they are much weaker than the corresponding ones in Tables II, III. Analogous conclusions hold for the bounds on $\xi_{\rm LQ}^3$. In particular we have not found any competitive process (with respect to $\mu-e$ conversion or $\mu\to 3e$) which can set better or comparable constraints on the $\xi_{\rm LQ}^3$ variables.

TABLE IV. Numerical upper bounds for the vectorial and scalar $SU(2)_L$-*singlet*-LQ variables $\xi^{ei}_{\mathrm{LQ}}\equiv|\lambda^{3i}_{\mathrm{LQ}}\lambda^{1i}_{\mathrm{LQ}}|\times(10^2\ \mathrm{GeV}/m_{\mathrm{LQ}})^2<(\xi^{ei}_{\mathrm{LQ}})^B$ and $\xi^{\mu i}_{\mathrm{LQ}}\equiv|\lambda^{3i}_{\mathrm{LQ}}\lambda^{2i}_{\mathrm{LQ}}|\times(10^2\ \mathrm{GeV}/m_{\mathrm{LQ}})^2<(\xi^{\mu i}_{\mathrm{LQ}})^B$ obtained from the experimental upper limits on the $\tau\to\pi^0 e$, $\tau\to 3e$ and $\tau\to\pi^0\mu$, $\tau\to 3\mu$, respectively. In the $\tau\to e\gamma$ and $\tau\to\mu\gamma$ rows, the variables which are constrained are $\tilde{\xi}^{ei}_{\mathrm{LQ}}\equiv\sqrt{|\lambda^{3i}_{\mathrm{LQ}}\lambda^{1i}_{\mathrm{LQ}}|}\times(10^2\ \mathrm{GeV}/m_{\mathrm{LQ}})^2<(\xi^{ei}_{\mathrm{LQ}})^B$ and $\tilde{\xi}^{\mu i}_{\mathrm{LQ}}\equiv\sqrt{|\lambda^{3i}_{\mathrm{LQ}}\lambda^{2i}_{\mathrm{LQ}}|}\times(10^2\ \mathrm{GeV}/m_{\mathrm{LQ}})^2<(\xi^{ei}_{\mathrm{LQ}})^B$, respectively. Note that the symbol $--$ stands for weaker constraints, see the text. Everywhere $(\xi^{e2}_{\mathrm{LQ}})^B=(\xi^{e3}_{\mathrm{LQ}})^B$ and $(\xi^{\mu 2}_{\mathrm{LQ}})^B=(\xi^{\mu 3}_{\mathrm{LQ}})^B$

Vector	i	$(\xi^{ei}_{LV_0})^B$	$(\xi^{ei}_{RV_0})^B$	$(\xi^{ei}_{R\tilde{V}_0})^B$
$\tau\to\pi^0 e$	1	1.9×10^{-3}	1.9×10^{-3}	1.9×10^{-3}
$\tau\to 3e$	2,3	3.3×10^{-1}	3.3×10^{-1}	1.0×10^{-1}
$\tau\to e\gamma$	2,3	$--$	$--$	5.7×10^{-2}
Vector	i	$(\xi^{\mu i}_{LV_0})^B$	$(\xi^{\mu i}_{RV_0})^B$	$(\xi^{\mu i}_{R\tilde{V}_0})^B$
$\tau\to\pi^0\mu$	1	1.9×10^{-3}	1.9×10^{-3}	1.9×10^{-3}
$\tau\to 3\mu$	2,3	2.7×10^{-1}	2.7×10^{-1}	8.3×10^{-2}
$\tau\to\mu\gamma$	2,3	$--$	$--$	5.8×10^{-2}
Scalar	i	$(\xi^{ei}_{LS_0})^B$	$(\xi^{ei}_{RS_0})^B$	$(\xi^{ei}_{R\tilde{S}_0})^B$
$\tau\to\pi^0 e$	1	3.7×10^{-3}	3.7×10^{-3}	3.7×10^{-3}
$\tau\to 3e$	2,3	2.0×10^{-1}	2.0×10^{-1}	6.6×10^{-1}
$\tau\to e\gamma$	2,3	7.7×10^{-2}	7.7×10^{-2}	1.5
Scalar	i	$(\xi^{\mu i}_{LS_0})^B$	$(\xi^{\mu i}_{RS_0})^B$	$(\xi^{\mu i}_{R\tilde{S}_0})^B$
$\tau\to\pi^0\mu$	1	3.9×10^{-3}	3.9×10^{-3}	3.9×10^{-3}
$\tau\to 3\mu$	2,3	1.7×10^{-1}	1.7×10^{-1}	5.3×10^{-1}
$\tau\to\mu\gamma$	2,3	7.9×10^{-2}	7.9×10^{-2}	1.6

In Tables IV, V we give the results for the corresponding bounds in the τ sector. In this case two new variables $\xi^{ei}_{\mathrm{LQ}}\equiv|\lambda^{3i}_{\mathrm{LQ}}\lambda^{ei}_{\mathrm{LQ}}|\times(10^2\ \mathrm{GeV}/m_{\mathrm{LQ}})^2$ and $\xi^{ei}_{\mathrm{LQ}}\equiv|\lambda^{3i}_{\mathrm{LQ}}\lambda^{ei}_{\mathrm{LQ}}|\times(10^2\ \mathrm{GeV}/m_{\mathrm{LQ}})^2$ (and analogous generalizations of the $\tilde{\xi}^{i}_{\mathrm{LQ}}$ variables, introduced in the μ sector, like $\tilde{\xi}^{ei}_{\mathrm{LQ}}$ and $\tilde{\xi}^{\mu i}_{\mathrm{LQ}}$) are defined. The ξ^{e1}_{LQ} and ξ^{e2}_{LQ} are more strongly constrained by the processes $\tau\to\pi^0 e$ and $\tau\to\pi^0\mu$ [24] whose effective Hamiltonians are induced at tree level by the LQs. In particular for a four-fermion vertex of the form

$$\frac{\lambda^{31}_{\mathrm{LQ}}\lambda^{l1}_{\mathrm{LQ}}}{m^2_{\mathrm{LQ}}}(\bar{l}\gamma^{\mu}P^{l}\tau)(\bar{q}_1\gamma^{\mu}P^{q}q_1), \tag{16}$$

one obtains[9] [10]

$$\xi^{l1}_{\mathrm{LQ}}<2\sqrt{2}(G_F\times(10^2\ \mathrm{GeV})^2)\cos\theta_c\sqrt{\frac{B^{\mathrm{exp}}_R(\tau^-\to\pi^0 l^-)}{B^{\mathrm{exp}}_R(\tau^-\to\pi^-\nu)}}, \tag{17}$$

where $q_1=U,D$ quarks, θ_c is the Cabibbo angle, $l=e,\mu$, and the central values of the experimental branching ratio is $B^{\mathrm{exp}}_R(\tau\to\pi^-\nu)=11.08\%$ [24]. The bounds in the $i=2,3$ sectors can be simply obtained by rescaling the corresponding ones in the μ sector in Tables IV, V by means of Eqs. (6), (11). In obtaining these bounds the following experimental upper limits at 90% C.L. have been used [24]: $B^{\mathrm{exp}}_R(\tau\to\pi^0 e)<3.7\times10^{-6}$, $B^{\mathrm{exp}}_R(\tau\to\pi^0\mu)<4\times10^{-6}$, $B^{\mathrm{exp}}_R(\tau\to 3e)<2.9\times10^{-6}$, $B^{\mathrm{exp}}_R(\tau\to 3\mu)<1.9\times10^{-6}$, $B^{\mathrm{exp}}_R(\tau\to e\gamma)<2.7\times10^{-6}$, and $B^{\mathrm{exp}}_R(\tau\to\mu\gamma)<3.0\times10^{-6}$. Because of a much lower experimental sensitivity in the τ branching ratios, we see that the bounds in Tables IV, V are between three and four orders of magnitude weaker than the corresponding ones in the μ sector.

[9]In obtaining Eq. (17) the following approximations for the matrix elements have been used [10]: $\langle 0|\bar{u}\gamma^{\mu}\gamma_5 u|\pi^0\rangle\simeq\langle 0|\bar{d}\gamma^{\mu}\gamma_5 d|\pi^0\rangle\simeq\langle 0|\bar{d}\gamma^{\mu}\gamma_5 u|\pi^+\rangle$.

TABLE V. Numerical bounds as in Table IV which here are relative to the $SU(2)_L$-*doublet*- and $SU(2)_L$-*vector*-LQs.

Vector	i	$(\xi^{ei}_{LV_{1/2}})^B$	$(\xi^{ei}_{RV_{1/2}})^B$	$(\xi^{ei}_{L\tilde{V}_{1/2}})^B$	$(\xi^{ei}_{LV_1})^B$
$\tau\to\pi^0 e$	1	1.9×10^{-3}	9.3×10^{-4}	1.9×10^{-3}	6.2×10^{-4}
$\tau\to 3e$	2,3	3.3×10^{-1}	1.5×10^{-1}	1.0×10^{-1}	6.1×10^{-2}
$\tau\to e\gamma$	2,3	2.8	9.8×10^{-2}	9.8×10^{-2}	4.0×10^{-2}
Vector	i	$(\xi^{\mu i}_{LV_{1/2}})^B$	$(\xi^{\mu i}_{RV_{1/2}})^B$	$(\xi^{\mu i}_{L\tilde{V}_{1/2}})^B$	$(\xi^{\mu i}_{LV_1})^B$
$\tau\to\pi^0\mu$	1	1.9×10^{-3}	9.7×10^{-4}	1.9×10^{-3}	6.4×10^{-4}
$\tau\to 3\mu$	2,3	2.7×10^{-1}	1.2×10^{-1}	8.3×10^{-2}	4.9×10^{-2}
$\tau\to\mu\gamma$	2,3	2.9	1.0×10^{-1}	1.0×10^{-1}	4.1×10^{-2}
Scalar	i	$(\xi^{ei}_{LS_{1/2}})^B$	$(\xi^{ei}_{RS_{1/2}})^B$	$(\xi^{ei}_{L\tilde{S}_{1/2}})^B$	$(\xi^{ei}_{LS_1})^B$
$\tau\to\pi^0 e$	1	3.7×10^{-3}	1.9×10^{-3}	3.7×10^{-3}	1.2×10^{-3}
$\tau\to 3e$	2,3	2.0×10^{-1}	3.0×10^{-1}	6.6×10^{-1}	5.5×10^{-1}
$\tau\to e\gamma$	2,3	5.7×10^{-2}	5.7×10^{-2}	1.7	7.7×10^{-2}
Scalar	i	$(\xi^{\mu i}_{LS_{1/2}})^B$	$(\xi^{\mu i}_{RS_{1/2}})^B$	$(\xi^{\mu i}_{L\tilde{S}_{1/2}})^B$	$(\xi^{\mu i}_{LS_1})^B$
$\tau\to\pi^0\mu$	1	3.9×10^{-3}	1.9×10^{-3}	3.9×10^{-3}	1.3×10^{-3}
$\tau\to 3\mu$	2,3	1.7×10^{-1}	2.4×10^{-1}	5.3×10^{-1}	4.4×10^{-1}
$\tau\to\mu\gamma$	2,3	5.8×10^{-2}	5.8×10^{-2}	1.8	7.9×10^{-2}

We discuss now the improvements of the LQ bounds in the muon sector which could be reached at the present and future muon experiments. In this respect it is convenient to introduce the *improvement* factor $B=\sqrt{\mathrm{BR}^{\mathrm{exp}}_{\mathrm{curr}}/\mathrm{BR}^{\mathrm{exp}}_{\mathrm{fut}}}$, where $\mathrm{BR}^{\mathrm{exp}}_{\mathrm{curr}}$ and BR^{exp}_{fut} are the current and future upper limits on the branching ratios, respectively. In the $\mu\to e\gamma$ sector the new bounds are obtained by dividing the current ones by $\sqrt{B}$ while in the $\mu\to 3e$ or $\mu-e$ conversion they should be divided by B. In the sector of the experimental searches for $\mu^+\to e^+\gamma$ it seems feasible, by using polarized muons (which are useful for suppressing the backgrounds [30]), to reach the sensitivity of about 10^{-14} on the branching ratio [31]. This is converted into an improvement factor $\sqrt{B}\simeq 8$ for the bounds from $\mu\to e\gamma$. The final analysis of the current SINDRUM II experiment at Paul Scherrer Institute (PSI) on the μ-e conversion [32] will reach a sensitivity of 10^{-14} on the branching ratio. This will give an improvement factor $B\simeq 8$ in the new bounds from the $\mu-e$ conversion.

A recent proposal for the μ-e conversion experiment (MECO) [33] at Brookhaven National Laboratory (BNL) will permit a sensitivity on the branching ratio better than 10^{-16}. This sensitivity is translated into an improvement factor $B\simeq 80$ for the LQ bounds from the μ-e conversion. In the context of the $\mu\to 3e$ decay (apparently) there is not any proposal, at the present and future muon facilities machines, for improving the sensitivity on this branching ratio.

V. CONCLUSIONS

In this article we perform a model-independent analysis so as to constrain the LQ models (B and L conserving) in the sector of rare FC leptonic processes; this is done by means of the $\mu \to e\gamma$, $\mu \to 3e$ decays (and analogous decays in the τ sector) and the μ-e conversion in nuclei. In our analysis we assume that the LQ couplings $\lambda_{\mathrm{LQ}}^{l_i q_j}$ (where l_i and q_j indicate the generation numbers of lepton and quarks, respectively) are unitary and real matrices. In order to set bounds on the LQ couplings and masses we find it convenient to introduce the following variables: $\xi_{\mathrm{LQ}}^{i} = |\lambda_{\mathrm{LQ}}^{2i}\lambda_{\mathrm{LQ}}^{1i}| \times (10^2 \ \mathrm{GeV}/m_{\mathrm{LQ}})^2$ in the μ sector, $\xi_{\mathrm{LQ}}^{ei} = |\lambda_{\mathrm{LQ}}^{3i}\lambda_{\mathrm{LQ}}^{1i}| \times (10^2 \ \mathrm{GeV}/m_{\mathrm{LQ}})^2$ and $\xi_{\mathrm{LQ}}^{\mu i} = |\lambda_{\mathrm{LQ}}^{3i}\lambda_{\mathrm{LQ}}^{2i}| \times (10^2 \ \mathrm{GeV}/m_{\mathrm{LQ}})^2$ in the τ one.

The μ-e conversion in nuclei, as shown in [10], is the best process for constraining the FC leptoquark couplings involving the first generation of quarks, namely the ξ_{LQ}^{1}, this is because the relevant effective Hamiltonian is induced at tree-level. The couplings involving the second and third quark generations can also be constrained by means of the one-loop contributions to the $\mu \to e\gamma$, $\mu \to 3e$ decays, and the $\mu - e$ conversion in nuclei. We show that the best of these processes to strongly constrain the variables $\xi_{\mathrm{LQ}}^{2,3}$ are the $\mu \to 3e$ and the $(\mu\text{-}e)_{\mathrm{Ti}}$. On the contrary the $\mu \to e\gamma$ decay can set much weaker constraints. This is because the former receive large logarithms $[\log(m_q/m_{\mathrm{LQ}})]$ enhancements at the amplitude level while the latter does not. In particular the $\mu \to 3e$ decay and μ-e conversion in nuclei (mediated by the photon-conversion mechanism) get the leading contributions from the so-called photon-penguin diagrams which, in the large LQ mass limit, are proportional to $\lambda_{\mathrm{LQ}}^2/m_{\mathrm{LQ}}^2 \times \log(m_q/m_{\mathrm{LQ}})$. On the other hand, the amplitude of the $\mu \to e\gamma$ is proportional (in the large LQ mass limit) to $\lambda_{\mathrm{LQ}}^2 m_q^2/m_{\mathrm{LQ}}^4$. The same considerations regarding the log enhancements hold for the corresponding processes in the τ sector.

The log enhancements in the photon-penguins are known in the literature [15,16], but they have not been applied in this context. In particular in the analysis of Ref. [10] these diagrams were not taken into account. As a consequence, in Ref. [10], the $\mu \to 3e$ branching ratio has been by far underestimated. Moreover, in Ref. [10] the scalar LQ couplings were not assumed to be unitary, thus allowing for large scalar LQ contributions to the $\mu \to e\gamma$ branching ratio.

The complete list of the bounds which we establish can be found in Tables II–V in both the μ and τ sectors. We next briefly outline the general trend of our results and describe the impact of the future experimental sensitivities on the muon branching ratios on our bounds.

The best constraints on all the ξ_{LQ}^{i} variables that we establish come from the current experimental upper limit on the $(\mu\text{-}e)_{Ti}$ branching ratio [27]. In particular, in both scalar and vectorial LQ sectors, the strongest bounds on ξ_{LQ}^{1} are at the level of $\xi_{\mathrm{LQ}}^{1} < 10^{-7}$ while the strongest bounds on $\xi_{\mathrm{LQ}}^{2,3}$ are weaker and are at the level of $\xi_{\mathrm{LQ}}^{2,3} < 10^{-5}$. The current experimental upper limits on the $\mu \to 3e$ decay can also set strong constraints on the $\xi_{\mathrm{LQ}}^{2,3}$ variables; however they are roughly a factor 5 weaker with respect to the corresponding ones in the μ-e sector.

The bounds obtained from the $\mu \to 3e$ decay can be calculated with high accuracy in perturbation theory, whereas the corresponding ones from the μ-e conversion in nuclei suffer from the problem of model-dependent calculations in the nuclear sector.

Because of a lower sensitivity in the τ experimental branching ratios [24], the bounds obtained from the rare τ decays are roughly four orders of magnitude weaker than the bounds in the μ sector. In particular the best bounds on ξ_{LQ}^{e1} and $\xi_{\mathrm{LQ}}^{\mu 1}$ are at the level of $\xi_{\mathrm{LQ}}^{\mu 1} < 10^{-3}$ and are set by the decays $\tau \to \pi^0 e$ and $\tau \to \pi^0 \mu$, respectively. The best bounds on $\xi_{\mathrm{LQ}}^{e(2,3)}$ and $\xi_{\mathrm{LQ}}^{\mu(2,3)}$ come from the $\tau \to 3e$ and $\tau \to 3\mu$ decays, respectively, and are at the level of $O(10^{-1})$.

Ultimately the current experiment on the $(\mu - e)_{Ti}$ conversion at PSI [27,31] will reach a sensitivity on the branching ratio that will enable us to improve the bounds in Tables II, III by a factor $\simeq 8$. However a new proposal (called MECO) for the $(\mu\text{-}e)_{Ti}$ conversion at BNL [33] could reach a sensitivity on the branching ratio that will considerably improve the bounds in Tables II, III by a factor $\simeq 80$.

ACKNOWLEDGMENTS

We gratefully acknowledge discussions with A. De Rujula, C. Di Cairano, B. Gavela, G. Isidori, C. Munoz, L. Silvestrini, A. Van der Schaaf, and D. Zanello. I acknowledge the financial support of the TMR network, project ‘‘Physics beyond the standard model,’’ FMRX-CT96-0090 and the partial financial support of the CICYT project Ref. AEN97-1678.

APPENDIX

We here give the analytical expressions for the functions $\Delta_{S,V}(x_t, Q)$ which appear in the branching ratios in Eqs. (4), (5), where $x_t = m_t^2/m_{\mathrm{LQ}}^2$ and Q can be $Q = R_{\mathrm{LQ}}$ or $Q = -R_{\mathrm{LQ}}$, with $R_{\mathrm{LQ}} \equiv Q_{\mathrm{LQ}}/Q_U$. In Eqs. (4), (5) the dependence by Q takes only two values, namely $Q = (1/2, -5/2)$. These functions, which are of order $O(x)$, take into account the exact dependence on the top mass in the photon-penguin diagrams and give the percentage difference between the leading logarithm approximation [which consists of neglecting the terms of order $O(x_t)$ with respect to $\log(x_t)$] and the exact result. Their expressions are given by

$$\Delta_V(x,Q) = \frac{x(-18+11x+x^2+Q(-12-x+7x^2))}{8(1-x)^3\log(x)} - \frac{x^2(15-16x+4x^2+Q(12-10x+x^2))}{4(x-1)^4},$$

$$\Delta_S(x,Q) = \frac{x(-19+41x-16x^2+Q(-1+5x+2x^2))}{12(x-1)^3\log(x)} - \frac{x(-5+12x+(Q-8)x^2+2x^3)}{2(x-1)^4}. \tag{A1}$$

In order to estimate the reliability of the leading log approximation, in Figs. 2, 3 we plot the absolute values of above functions versus the leptoquark mass in both the scalar and vectorial cases.

[1] J. C. Pati and A. Salam, Phys. Rev. D **10**, 275 (1974); P. Langacker, Phys. Rep. **72**, 185 (1981); H. Georgi and S. L. Glashow, Phys. Rev. Lett. **32**, 438 (1974).

[2] A. Dobado, M. J. Herrero, and C. Muñoz, Phys. Lett. B **191**, 449 (1987).

[3] B. A. Campbell *et al.*, Int. J. Mod. Phys. A **2**, 831 (1987); J. F. Gunion and E. Ma, Phys. Lett. B **195**, 257 (1987); R. Robinett, Phys. Rev. D **37**, 1321 (1988); J. Hewett and T. Rizzo, Phys. Rep. **183**, 193 (1989); J. A. Grifols and S. Peris, Phys. Lett. B **201**, 287 (1988); E. Halyo, *ibid.* **326**, 251 (1994).

[4] B. Schrempp and F. Schrempp, Phys. Lett. B **153**, 101 (1985); J. Wudka, Phys. Lett. B **167**, 337 (1986).

[5] S. Dimopoulos and L. Susskind, Nucl. Phys. **B155**, 237 (1979); S. Dimopoulos, *ibid.* **B168**, 69 (1980); E. Farhi and L. Susskind, Phys. Rev. D **20**, 3404 (1979); Phys. Rep. **74**, 277 (1981), and references therein.

[6] W. Buchmuller, R. Rückl, and D. Wyler, Phys. Lett. B **191**, 442 (1987); **448**, 320(E) (1999).

[7] For a review on leptoquarks at HERA, see R. J. Cashmore *et al.*, Phys. Rep. **122**, 275 (1985).

[8] O. Shanker, Nucl. Phys. **B204**, 375 (1982); R. Mohapatra, G. Segré, and L. Wolfenstein, *ibid.* **B145**, 433 (1984); I. Bigi, G. Köpp, and P. M. Zerwas, *ibid.* **B166**, 238 (1986); B. A. Campbell *et al.*, Int. J. Mod. Phys. A **2**, 831 (1987); A. J. Davies and X. He, Phys. Rev. D **43**, 225 (1991).

[9] M. Leurer, Phys. Rev. Lett. **71**, 1324 (1993); Phys. Rev. D **49**, 333 (1994); **50**, 536 (1994).

[10] S. Davidson, D. Bailey, and B. A. Campbell, Z. Phys. C **61**, 613 (1994), and references therein.

[11] G. Altarelli, J. Ellis, G. F. Giudice, S. Lola, and M. L. Mangano, Nucl. Phys. **B506**, 3 (1997); G. Altarelli, G. F. Giudice, and M. L. Mangano, *ibid.* **B506**, 29 (1997); K. S. Babu, C. Kolda, J. March-Russell, and F. Wilczek, Phys. Lett. B **402**, 367 (1997); C. Friberg, E. Norrbin, and T. Sjostrand, *ibid.* **403**, 329 (1997); M. Heyssler and W. J. Stirling, *ibid.* **407**, 259 (1997); J. L. Hewett and T. G. Rizzo, Phys. Rev. D **56**, 5709 (1997); E. Keith and E. Ma, Phys. Rev. Lett. **79**, 4318 (1997); T. K. Kuo and T. Lee, Mod. Phys. Lett. A **12**, 2367 (1997); T. Plehn, H. Spiesberger, M. Spira, and P. M. Zerwas, Z. Phys. C **74**, 611 (1997); Z. Kunszt and W. J. Stirling, *ibid.* **75**, 453 (1997); N. G. Deshpande and B. Dutta, Phys. Lett. B **424**, 313 (1998); J. K. Elwood and A. E. Faraggi, Nucl. Phys. B **512**, 42 (1998); M. Sekiguchi, H. Wada, and S. Ishida, Prog. Theor. Phys. **99**, 707 (1998).

[12] H1 Collaboration, C. Adloff *et al.*, Z. Phys. C **74**, 191 (1997).

[13] ZEUS Collaboration, J. Breitweg *et al.*, Z. Phys. C **74**, 207 (1997).

[14] H1 Collaboration, C. Adloff *et al.*, Eur. Phys. J. C **11**, 447 (1999).

[15] W. J. Marciano and A. L. Sanda, Phys. Rev. Lett. **38**, 1512 (1977).

[16] M. Raidal and A. Santamaria, Phys. Lett. B **421**, 250 (1998).

[17] S. Weinberg and G. Feinberg, Phys. Rev. Lett. **3**, 111 (1959); **3**, 244(E) (1959); N. Cabibbo and R. Gatto, Phys. Rev. **116**, 1334 (1959); S. P. Rosen, Nuovo Cimento **15**, 7 (1960).

[18] O. Shanker, Phys. Rev. D **20**, 1608 (1979).

[19] A. Czarnecki, W. J. Marciano, and K. Melnikov, hep-ph/9801218; Proceedings of the Workshop on Physics at the First Muon Collider and at the Front End of the Muon Collider, edited by S. Geer and R. Raja, Batavia, Illinois, 1997, p. 409; also see in Batavia 1997, Physics at the First Muon Collider, pp. 409–418.

[20] H. C. Chiang *et al.*, Nucl. Phys. A **559**, 526 (1993).

[21] T. S. Kosmas, A. Faessler, F. Simkovic, and J. D. Vergados, Phys. Rev. C **56**, 526 (1997); T. S. Kosmas, A. Faessler, and J. D. Vergados, J. Phys. G **23**, 693 (1997).

[22] K. Huitu, J. Maalampi, M. Raidal, and A. Santamaria, Phys. Lett. B **430**, 355 (1998).

[23] S. Bertolini, F. Borzumati, A. Masiero, and G. Ridolfi, Nucl. Phys. **B353**, 591 (1991).

[24] Particle Data Group, C. Caso *et al.*, Eur. Phys. J. C **3**, 1 (1998).

[25] E. Gabrielli and G. F. Giudice, Nucl. Phys. **B433**, 3 (1995); **B507**, 549(E) (1997).

[26] Y. Okada, K. Okumura, and Y. Shimizu, Phys. Rev. D **61**, 094001 (2000); Y. Kuno and Y. Okada, hep-ph/9909265.

[27] ''Search for $\mu^- \to e^-$ Conversion on Titanium,'' SINDRUM II Collaboration, S. Eggli *et al.*, 1999; P. Wintz, in *Proceedings Lepton-Baryon 98*, edited by H. V. Klapdor-Kleingrothaus and I. V. Krivosheina (IOP, Bristol, 1999), p. 534.

[28] E. Gabrielli (in preparation).

[29] MEGA Collaboration, M. L. Brooks *et al.*, Phys. Rev. Lett. **83**, 1521 (1999).

[30] Y. Kuno and Y. Okada, Phys. Rev. Lett. **77**, 434 (1996); Y. Kuno, A. Maki, and Y. Okada, Phys. Rev. D **55**, 2517 (1997); A. Czarnecki, *5th International Conference Beyond the Standard Model*, Balholm, Norway, 1997, p. 252, hep-ph/9710425.

[31] M. Felcini *et al.*, ''A search for the decay $\mu^+ \to e^+ \gamma$ with a branching ratio sensitivity of 10^{-14},'' LOI for an experiment at PSI (1998).

[32] A. Van der Schaaf (private communications).

[33] M. Bachman *et al.*, ''A search for the decay $\mu N \to e N$ with sensitivity below 10^{-16} MECO,'' Proposal to Brookhaven National Laboratory AGS (1997).